



Australian Government

REC'D 06 APR 2004

WIPO PCT

# PRIORITY DOCUMENT

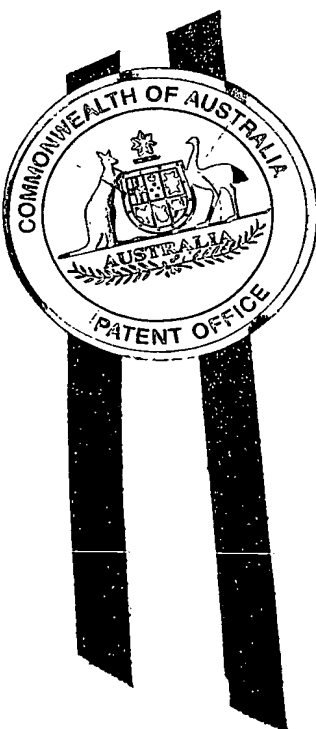
SUBMITTED OR TRANSMITTED IN  
COMPLIANCE WITH RULE 17.1(a) OR (b)

Patent Office  
Canberra

I, JULIE BILLINGSLEY, TEAM LEADER EXAMINATION SUPPORT AND SALES hereby certify that annexed is a true copy of the Provisional specification in connection with Application No. 2003901269 for a patent by VICTOR CHANG CARDIAC RESEARCH INSTITUTE LIMITED as filed on 19 March 2003.

WITNESS my hand this  
Thirty-first day of March 2004

JULIE BILLINGSLEY  
TEAM LEADER EXAMINATION  
SUPPORT AND SALES



BEST AVAILABLE COPY

**AUSTRALIA**

***Patents Act 1990***

**Victor Chang Cardiac Research Institute Limited**

**PROVISIONAL SPECIFICATION**

**Invention Title:**

**Model for muscular dystrophy**

**The invention is described in the following statement:**

Technical Field

The present invention relates to zebrafish models for studying muscular dystrophy in mammals. The invention is also suitable for screening agents which may have an affect on the clinical manifestations of muscular dystrophy.

5

Background Art

Genetic lesions within the structural muscle protein Dystrophin lead to the onset of the fatal muscle wasting diseases, Becker (BMD) and Duchenne (DMD) muscular dystrophies, as well as other dystrophinopathies in humans. Dystrophin is associated 10 with a number of glycoproteins which span the sarcolemma of skeletal and cardiac muscle to form the Dystrophin-glycoprotein complex. Although the exact role that this complex plays in muscle physiology is not fully understood, it is thought that it provides an important structural link between the cytoskeleton and the extracellular matrix of muscle cells. This connection is theorised to be critical in regulating stresses that 15 develop during muscle contraction. The lack of Dystrophin in DMD patients results in a reduction in all of the components of the Dystrophin-glycoprotein complex and a breakage in this transmembrane linkage. A weakening of the muscle membrane results, which consequently manifests itself in the pathological features of DMD. A number of diagnostic features of DMD become evident including cycles of muscle cell necrosis and 20 regeneration, and elevated levels of muscle creatine kinase. At an advanced stage of the disease muscle is replaced by connective tissue and fat. Consequently, DMD afflicted individuals suffer from progressive muscular wasting and usually die before the age of 20 from respiratory or cardiac failure.

Research into the events that determine the human dystrophic pathology has 25 benefited from the generation of mice mutant in the mouse *Dystrophin* gene *mdx*. However, despite *mdx* mutant mice demonstrating a number of phenotypic hall marks of muscular dystrophy early in their development, adult *mdx* mice show little muscle weakness and live near normal life spans, a consequence, perhaps, of the substantial muscle regeneration evident within these mice post weaning. The lack of similarity 30 between the mouse model and the human disease has hampered research into the function of dystrophin in maintaining muscle integrity. Other large animal models such as dystrophic dogs have also been identified, but their large size and generation times make them highly unsuitable laboratory models.

The present inventors have identified genes and mutations in zebrafish which correspond to mammalian genes which have been implicated in muscular dystrophy and have developed a fish model for muscular dystrophy. The model is highly penetrant and presents with many of the hall marks of the human disease. In short the zebrafish 5 laboratory dystrophic model overcomes the major short coming of mammalian models in terms of disease penetrance and manipulability of a laboratory model system

#### Disclosure of Invention

In a first aspect, the present invention provides isolated zebrafish genetic strain 10 having a dystrophin mutant phenotype.

Preferably, the mutant has a *sapre* phenotype as defined herein.

Large-scale mutagenic screens of the zebrafish genome have identified numerous mutations that disrupt differentiation and maintenance of skeletal muscle within the zebrafish embryo. Mutants possess phenotypes that range from a failure of 15 myoblasts to elongate and fuse into multinucleate muscle fibres to those that exhibit muscle degeneration reminiscent of human muscular dystrophies. Homozygous mutants of this latter class form myofibrils normally but are lost focally or globally, depending on the loci involved, during early larval life. One member of the zebrafish dystrophic mutant class has its phenotype resulting from mutations within the zebrafish 20 dystrophin orthologue. A detailed characterisation of the phenotype that arises as a consequence of the loss of dystrophin expression within the embryonic and larval myotomes of zebrafish has been carried out. This analysis points to the critical and novel roles that the dystrophin and its associated-glycoprotein complex plays in the ontogeny of zebrafish muscle. The function of dystrophin in teleost and mammalian 25 muscle fibre biogenesis has been compared. This analysis represents the first identification of a zebrafish model of a human muscular dystrophy and has applications to the study of the human dystrophic condition.

Preferred mutants are *sapre* *tm90c*, *tj7*, *ta222a*.

It will be appreciated that further mutants, progeny, fry, gametes are also 30 included.

In a second aspect, the present invention provides a fish model of mammalian muscular dystrophy comprising an isolated zebrafish according to the first aspect of the present invention.

Preferably, the model is of human muscular dystrophy.

In a third aspect, the present invention provides a method for screening agents having potential activity on muscular dystrophy comprising:

- (a) providing a fish model according to the second aspect of the present invention;
- 5 (b) exposing the zebrafish to an agent; and
- (c) determining any affect of the agent on a genetic or physical characteristic of the zebrafish or its progeny.

The agent may be a drug candidate, chemical, nucleic acid and the like.

10 The agent may be administered by direct dilution in raising media, or direct administration to the fish by any suitable means.

The affect may be determined by any visual or light microscopic technique including those that utilise transgenic reporter gene expression to monitor muscle integrity.

15 In a fourth aspect, the present invention provides an agent determined to have activity on muscular dystrophy by the method according to the third aspect of the present invention.

In a fifth aspect, the present invention provides a method for monitoring or testing the effect of an agent having activity on muscular dystrophy comprising:

- (a) providing a fish model according to the second aspect of the present invention;
- 20 (b) exposing the zebrafish to the agent; and
- (c) monitoring the effect of the agent on a genetic or physical characteristic of the zebrafish or its progeny.

25 The present inventors have identified a class of zebrafish mutations as candidates for mutations in human muscular dystrophy disease genes. The molecular lesion in one of these mutations, *sapjre* has been identified. The *sapjre* phenotype resulted from mutations within the dystrophin gene, human mutations in which result in Becker's and Duchenne Muscular Dystrophy, the most common forms of muscular dystrophy.

30 The present research has established a formal link between the phenotype of this particular class of zebrafish mutations and human muscular dystrophies. The phenotypes of these mutations have been characterised in detail, including that of the *sapjre* mutation analysed in the results section below. These mutations exhibit muscle

weakness in a similar manner to that described to occur in human patients. The phenotype of *sapre* (the zebrafish dystrophin mutation) has been characterised in the most detail. This phenotype results from a loss of membrane integrity on the inner membrane region, consistent with a failure of dystrophin to link from the actin cytoskeleton to the sarcolemma. This results in membrane tearing in an identical fashion to human muscle fibres deficient in dystrophin. The mutation has been mapped on the zebrafish genetic map, establishing linkage to dystrophin, assembled full-length zebrafish and fugu (pufferfish) dystrophin genes, and performed mutation detection on DNA derived from the homozygous *sapre* mutants. Stop codons have been identified within the zebrafish dystrophin open reading frame in *sapre* homozygotes. Antisense oligo-mediated knockdown of dystrophin results in an identical phenotype to that produced by the *sapre* mutation. It has also been found that the *sapre* phenotype results from a mutation in the zebrafish *dystrophin* gene.

The highly penetrant nature of the zebrafish dystrophin mutant phenotype more closely mirrors the human phenotype than that present in the MDX mouse model, suggesting it will be a very useful tool. A number of attributes of zebrafish biology and development lend themselves to the implementation of a high through out screening rationales for genetic and pharmacological modifiers of the dystrophic phenotype. External fertilisation, high fecundity, optical transparency and small size of the embryos will allow us to directly screen for chemicals or second site mutations that modulate the dystrophic phenotype. These findings would form the basis of drug design for treatment of the human dystrophic condition.

Throughout this specification, unless the context requires otherwise, the word "comprise", or variations such as "comprises" or "comprising", will be understood to imply the inclusion of a stated element, integer or step, or group of elements, integers or steps, but not the exclusion of any other element, integer or step, or group of elements, integers or steps.

Any discussion of documents, acts, materials, devices, articles or the like which has been included in the present specification is solely for the purpose of providing a context for the present invention. It is not to be taken as an admission that any or all of these matters form part of the prior art base or were common general knowledge in the field relevant to the present invention as it existed in Australia before the priority date of each claim of this application.

In order that the present invention may be more clearly understood, preferred forms will be described with reference to the following drawings and examples.

### Brief Description of the Drawings

Figure 1 *sap* mutants develop lesions in skeletal muscle where fibres detach from myosepta and retract. Wild-type (a, c, e, g) and *sap* (b, d, f, h). a, b lateral views, 48 hpf. Fibres in wild-type span the entire somite at between myosepta (arrowheads in a). Lesions within *sap* somites are evident as cell free spaces (arrowheads in b). c, d horizontal sections, 72hpf. Haematoxylin and eosin staining of reveals detached, rounded fibres in association with lesions in *sap* (arrowheads in d) but not in wild-type. e, f transverse sections, 72hpf. Anti-myosin heavy chain staining (green) reveals that the lesions in *sap* (f) somites lack contractile apparatus suggesting fibre loss (arrowheads). g, h lateral views of somites at 5dpf reconstructed in 3D using confocal microscopy. Somites expressing the skeletal muscle specific  $\alpha$ -actin::EGFP transgene appear intact in wild-type (g) but often show extensive fibre loss in *sap* (h.). Scale bars =80  $\mu$ m.

Figure 2 Dystrophin is associated with the wild-type embryonic myomuscular junction. a, b lateral views. *dystrophin* mRNA localises intracellularly to wild-type somite boundaries both before (19hpf, a) and after (27hpf, b) muscle fibre differentiation (arrowheads). A crescent of mRNA is present at one side of undifferentiated cells that abut somite boundaries. c-g Dystrophin protein is localised embryonically to fibre ends at somite boundaries (arrows in c-g, anti-dystrophin labelled green), and at NMJs but not at the sarcolemma. c, d horizontal sections, 72hpf. Dystrophin in fibre ends sandwiches the extracellular matrix of the vertical myoseptum at somite boundaries, which contains tenascin-C (arrowhead in d shows anti-tenascin-C labelled red, nuclei labelled blue with DAPI). e-g Dystrophin localises to MMJs and NMJs but not the sarcolemma embryonically. e transverse section, 72hpf. Dystrophin is detectable at MMJs (arrows) and as a punctate pattern within the myotome (arrowheads). f, g horizontal sections, 72hpf. Triple labelling using anti-dystrophin (green), Alexa594- $\alpha$ -Bungarotoxin to label NMJs (BTX, red), and DAPI (blue) reveals that dystrophin within the myotome is at NMJs, co-localising with BTX to producing an overlapping yellow signal. Scale bars =40  $\mu$ m.

Figure 3 *sap* is a mutation of *dmd* that causes loss of dystrophin from the MMJ and fibre detachment, and which is phenocopied by knocking down *dmd* function. a-c Dystrophin is localised to MMJs at somite boundaries in wild-type (a) but lacking in both *sap* (b) and dystrophin-morphant embryos (c) at 27hpf (lateral views). d, e By 72hpf, dystrophin is localised at the basal lamina around the neural tube in both wild-type and *sap* (arrows) but still lacking from MMJs (arrowheads) in *sap* (transverse sections). i, j

$\beta$ -dystroglycan is also localised to basal laminae in wild-type and *sap* at 72hpf (arrows), but unlike dystrophin is present at MMJs in both (arrowheads, transverse sections). f-h Evans blue dye, which is taken up by cells with compromised membranes (red fluorescence), does not appear in wild-type somites (f), but labels fibres in both *sap* (g) and dystrophin-morphant embryos (h). Labelled fibres are visible that have either both detached and retracted (arrowheads) or still span a somite (arrows, lateral views, 72hpf). Scale bars =80 $\mu$ m. k Partial alignment of zebrafish (Dr\_dys), predicted *Fugu rubripes* (Fr\_predict), human (Hs\_dys) and chicken (Gg\_dys) dystrophin proteins. The region shown includes two N-terminal calponin homology domains (CH, underlined), and is encoded by exons 2 to 7. The termination site of the *sap*<sup>tm90c</sup> form of zebrafish dystrophin is marked by an asterisk. Estimated positions of exon boundaries are marked by green arrowheads, except that between exons 6 and 7 (red arrowhead) against which morpholino MO1 was directed. l Rooted tree showing dystrophin and utrophin proteins in vertebrates. The tree is rooted using *Drosophila melanogaster* dystrophin. The numbers on each arm represent the percentage of 1000 bootstrap trials that support the branch. DYS, dystrophin; UTRO, utrophin, Hum, *Homo sapiens*; Dog, *Canis familiaris*; Mus, *Mus musculus*; Chick, *Gallus gallus*; Fugu, *Fugu rubripes*; Zebra, *Danio rerio*; Rat, *Rattus norvegicus*. Proteins accession numbers: Drosophila dystrophin, XP\_081212; Human dystrophin, NP\_000100; Dog dystrophin, O97592; Mouse dystrophin, NP\_031894; Chicken dystrophin, CAA31746, Human utrophin, NP\_009055; Mouse utrophin, CAA58496. The Fugu sequence is a manually corrected GENSCAN prediction from a genomic scaffold ([www.jgi.doe.gov/fugu](http://www.jgi.doe.gov/fugu), Scaffold 234). The tree has been made from partial sequences corresponding to the zebrafish protein published in this paper. m In 28 individual embryos tested, the nonsense mutation identified (AAA $\rightarrow$ TAA) in *dmd* segregates in the homozygous state exclusively with the *sap*<sup>tm90c</sup> phenotype.

Figure 4 *In vivo* observation of myomuscular junction failure and molecular analysis of detached free ends. a, b lateral view, 5dpf. A single fibre in the process of detaching from both anterior (left) and its posterior myosepta, under differential interference contrast (DiC, a) and labelled with EBD (b). A gap is visible between the posterior end of the fibre (short arrows) and the myoseptum (arrowheads). Wild-type (c) and *sap* mutant embryos (d) expressing an  $\alpha$ -actin::EGFP transgene viewed under confocal microscopy at 72hpf also shows the free end of a single newly detached fibre (d, bracket). The use of stacked confocal images allows the tracing of individual fibres to their insertion points at the MMJ. Detaching fibres within *sap* homozygotes (d) exhibit

a club-like or faceted appearance at their newly detached membranes, not evident in wild-type embryos (c). e, f  $\beta$ -DG protein at the MMJ is not present in the fibre membranes as detachment occurs. Two neighbouring mutant cells visible at 72hpf under DIC (e) are attached to the myoseptum (arrows) at their posterior ends but free at

5 their anterior (arrowheads). Labelling with anti- $\beta$ -DG (f) shows that this integral membrane protein has been lost during detachment from the anterior ends. g, h In wild-type and *sap*, cytoplasmic Focal Adhesion Kinase (FAK), viewed under confocal microscopy at 72hpf, is also enriched at the MMJ (arrows). Unlike  $\beta$ -DG, however, FAK remains visibly localised to the free end of detached cells as crescents, indicating  
 10 retention of terminal structures (arrowhead in h). Scale bars =80 $\mu$ m for a-f, =10  $\mu$ m for g, h.

**Mode(s) for Carrying Out the Invention**

**METHODS**

15 **Immunohistochemistry**

We carried out immunohistochemistry as previously described<sup>21</sup>. Anti-dystrophin MANDRA1 (Sigma) was diluted 1:1000. Anti- $\beta$ -DG (Novocastra) was diluted 1:10. Anti-MyHC A4.1025 (DSHB, University of Iowa) was used diluted 1:400. Appropriate Alexa-dye-labelled secondary antibodies (Molecular Probes) were used. Alexa-594- $\alpha$ -  
 20 Bungarotoxin and DAPI (Molecular Probes) were diluted 1:1000.

***In situ* hybridisation**

We carried out *in situ* hybridisation as previously described<sup>21</sup>.

25 **Evans Blue Dye labelling**

Evans Blue Dye (Sigma) was injected at 0.1 mg/ml<sup>-1</sup> directly into the pericardium of anaesthetised embryos, which were examined and photographed 4-6 hours later.

Confocal microscopy. We used a Zeiss LSM 510 confocal microscope and Zeiss software.

### Fish strains and maintenance

Complementation analysis of the dystrophic mutant class was carried out on mutations obtained from the Tübingen Stock Centre. In this analysis *sapje*<sup>tm90c</sup> and a second unnamed mutation, *ta222a* failed to complement. Subsequent analysis has 5 shown that extant stocks of both strains held in Edinburgh and Tübingen carry identical point mutations, suggesting that these different alleles may result from a single founder mutation within the original mutant screen. We therefore refer here to one mutation, *sapje*<sup>tm90c</sup>, although analysis was carried out on both strains.

### 10 Mapping

*dmd* was previously mapped using the LN54 radiation panel to between Z5508 and Z5085<sup>2</sup>. We established linkage between *sap* and *dmd* using Z5508 on individual embryos from a mapping cross versus the Wik strain.

### 15 Cloning of zebrafish *dmd* and identification of point mutation

Initial identification of zebrafish sequences was carried out by comparing human dystrophin Dp427m to the zebrafish whole genome shotgun. Exonic sequences were used to design primers for PCR from cDNA pools. We extracted mRNA from wild-type and mutant embryos using DynaBeads (Dynal) and made cDNA pools (Roche). 20 PCR products were cloned in pGem-T (Promega), sequenced, and assembled and compared using Sequencher.

### Morpholino

We purchased morpholino antisense oligonucleotide MO1 from GeneTools. We 25 prepared and injected solutions as described<sup>13</sup>.

### Sequence analysis

Sequences were aligned using CLUSTALW (v1.82 with default settings)<sup>22</sup>. Positions in alignments containing gaps were omitted from subsequent analyses. All 30 phylogenetic trees were constructed by the neighbour-joining method<sup>23</sup> based on the proportion of amino acid sites at which sequences compared were different. The reliability of each interior branch of a given topology was assessed using the bootstrap

interior branch test with 1000 bootstrap replications<sup>24</sup>. Phylogenetic trees were constructed using MEGA<sup>25</sup> (v2.1; <http://www.megasoftware.net/>) and alignments were examined and formatted in GeneDoc (v2.6.02; <http://www.psc.edu/biomed/genedoc/>). The *Fugu* data has been provided freely by the Fugu Genome Consortium for use in this publication/correspondence only.

5 Genbank Accession numbers: *Danio rerio* *dystrophin* (*dmd*) 5' sequence is AY162403 and *Fugu rubripes* *dystrophin* predicted 5' sequence is BK000643.

## RESULTS

10 Myotomal lesions are first evident in homozygous *sap* mutant embryos at 36 hours post fertilisation (hpf), after an initial period of muscle development within which muscle fibres elongate and striate normally within the myotome (Figure 1a, b). From this time, lesions in *sap* homozygous mutant embryos progressively accumulate until death occurs at larval stages (median =31 days post fertilisation (dpf), n=25).

15 Histological analysis revealed that fibres associated with lesions had detached from the vertical myosepta at the somite boundaries and are dramatically shortened (Figure 1c, d). An examination of the expression of myosin heavy chain (MyHC) within *sap* homozygous mutants confirms that fibre differentiation appears to occur in the correct spatial and temporal sequence within these embryos. However, lesions are

20 associated with fibre loss, producing MyHC negative gaps within the differentiated myotome (Figure 1e, f). The extent to which damage is sustained by individual mutant somites was examined using an  $\alpha$ -actin::EGFP transgene<sup>4</sup> under confocal microscopy. This revealed extensive fibre damage in some somites, whilst neighbouring areas remained almost unaffected, suggesting that variable factors such as motor activity may

25 contribute to degeneration (Figure 1g, h).

The similarity of the *sap* phenotype to muscular dystrophies led us to identify the zebrafish *dystrophin* (*dmd*) gene, revealing an intimate association of its expression with fibre ends. *dmd* mRNA becomes localised intracellularly towards somite boundaries before muscle fibre differentiation occurs and remains so throughout development

30 (Figure 2a, b), being subsequently concentrated at the ends of muscle fibres<sup>2</sup>. This pattern is preserved in *sap*. Dystrophin protein also localises in somitic muscle to the ends of fibres at the point where they attach to the vertical myoseptum (Figure 2c, d), which is a fibrous, cell free, sheet of extracellular matrix containing Tenascin-C (Figure 2d)<sup>5</sup>. This localisation persists until at least 6 dpf. Dystrophin was not

35 detectable at the embryonic sarcolemma before 6 dpf, however it is known to be present

within the adult sarcolemma<sup>8</sup>. Embryonically, dystrophin is detectable within the myotome, but colocalises entirely with neuromuscular junctions (NMJ, Figure 2e-g). Thus, the major site of embryonic dystrophin expression is the ends of muscle fibres where they attach via the vertical myoseptum to the fibres of the next somite, generating myomuscular junctions (MMJs)<sup>7</sup>.

*sap* mutants lack dystrophin immunoreactivity at muscle fibre ends, but retain later expression at sites outside the somites (Figure 3a, b, d, e), suggesting a selective loss of isoforms. This observation is consistent with the *sap* phenotype resulting from damage specific to the boundary regions of somitic muscle. Localisation of the transmembrane β-chain of the dystrophin-binding laminin receptor, dystroglycan (β-DG), which is required for muscle differentiation, is normal in *sap* (Figure 3i, j), indicating that dystrophin is not required for this process<sup>8,9</sup>. To investigate the effects of *sap* on membrane integrity at the MMJ, we injected Evans Blue Dye (EBD), which labels cells with compromised membranes<sup>10</sup>. EBD labels many detached fibres in *sap* somites (Figure 3f, g), and a few fibres that are still attached at both ends. Such labelling indicated that there was loss of membrane integrity when fibres detach their ends from myosepta<sup>10</sup>. Loss of dystrophin, retention of dystroglycan, and membrane damage all occur in Duchenne muscular dystrophy<sup>3</sup>, making *dmd* a strong candidate for *sap*.

Comparing the human dystrophin protein to the zebrafish whole genome shotgun reads using BLAST<sup>11</sup> identified fragments of a single gene, which we subsequently joined by PCR to recover cDNA sequences representing nearly the complete open reading frame. Comparisons of the N-terminal region with other species, including a predicted *Fugu* protein which we identified (Figure 3k, l), confirmed earlier findings that zebrafish *dmd* is the true orthologue of the human *DMD* gene<sup>6</sup>. *dmd* was previously mapped to Linkage Group 1 (LG1)<sup>2</sup>, and we used markers at this position to test for linkage to *sapje*<sup>tm90c</sup>. This revealed close linkage, and we therefore examined *sapje*<sup>tm90c</sup> for mutations in *dmd* (Figure 3k, m). The absence of dystrophin C-terminal immunoreactivity from *sap* muscle but not from other sites suggested that *sapje*<sup>tm90c</sup> might be a mutation in an exon of *dmd* retained exclusively at embryonic stages in muscle-specific isoforms. This and the large size of the human orthologue led us to initiate mutation detection within 5' exons of the zebrafish gene homologous to those present in Dp427m, the isoform of dystrophin that predominates in mammalian muscle. Within exon 4 of *dmd* from *sapje*<sup>tm90c</sup> we found an A→T transversion causing a nonsense mutation within the first calponin homology (CH) domain, which segregated in the homozygous state exclusively with the *sap* phenotype (Figure 3k, m). By comparison, a

nonsense mutation in exon 4 of human *DMD* causes DMD, indicating that this exon is essential in human muscle<sup>12</sup>. To confirm that this mutation causes the *sap* phenotype we injected an antisense morpholino oligonucleotide (MO1), targeted to overlap the boundary of zebrafish *dmd* exon 6 and its downstream intron, at the 1-cell stage. This 5 was predicted to produce exon-skipping<sup>13</sup> from exon 5 to exon 7, resulting in a frameshift and premature termination within exon 7, and its effectiveness was evidenced by the absence of dystrophin C-terminal immunoreactivity in injected embryos (Figure 3c). MO1 injections phenocopied *sap* (46/159, 29%), causing somitic EBD uptake and lesions that were never seen among embryos injected with control morpholinos 10 (Figure 3c, h). Thus, we conclude that the mutation in *dmd* causes the *sap*<sup>tm90c</sup> phenotype.

In order to understand the cellular basis for muscle degeneration present within *sap* homozygotes, we continuously monitored mutant somites using both light microscopy and EBD-labelling. EBD labels fibres prior to retraction and we were 15 consequently able to observe single mutant fibres *in vivo* detaching from myosepta (Figure 4a, b). This detachment is characterised by a progressive stretching and tearing from the myoseptum of fibre end membranes and a consequent failure of attachment at the MMJ. Consistent with these observations, utilising three-dimensional confocal microscopy to trace newly detached fibres along the entirety of their length revealed 20 morphological abnormalities specifically associated with the free fibre ends. Detached fibres often possessed a novel club-like or multifaceted appearance. Thus, the degeneration of muscle tissue in *sap* mutants occurs through failure of the MMJ with associated loss of membrane integrity. Our analysis of the phenotype of homozygous *sap* mutant embryos represents the first genetic evidence that dystrophin is required for 25 the formation of stable attachments at the end of vertebrate muscle fibres.

In order to determine precisely where detachment and membrane damage occur in *sap*, we examined the MMJ of *sap* mutants using immunohistochemistry to detect proteins normally localised either within the terminal membrane or immediately 30 intracellular to it. In *sap* mutants the transmembrane protein β-dystroglycan remains associated with the myoseptum when fibres detach, consistent with failure at the level of dystrophin, which lies immediately intracellular to the sarcolemma at the MMJ (Figure 4e, f). However, focal adhesion kinase (FAK), an integrin-associated 35 cytoplasmic protein enriched at the embryonic somite boundary, is retained in free the ends of detached fibres, also indicating that failure occurs near the plane of the sarcolemma. Therefore, membrane integrity is lost on the inner side of the plasma

membrane, consistent with a structural failure of dystrophin linkage between the actin cytoskeleton and the plasma membrane causing the observed detachments.

The pathology of Duchenne and other muscular dystrophies has been thought to result primarily from the loss of proteins of the DGC from the sarcolemma, leading to a loss of mechanical support between muscle fibres and membrane tearing during contraction<sup>3</sup>. However, dystrophin-deficient *mdx* mice recover from an acute phase of muscle fibre necrosis without sarcolemmal damage or permanent debilitation, perhaps because of efficient regeneration or compensation by the related protein utrophin<sup>14-17</sup>. Another possible reason for the mild phenotype of *mdx* mice could be that dystrophin is required at membrane specialisations such as muscle end attachments in humans but less so in mouse fibres.

Dystrophin is enriched both at mammalian myotendinous junctions (MTJs) and within large mammalian muscles at MMJs attaching fibres in series. Mammalian muscles more than a few centimetres long are arranged either as mingled overlapping fibres joined end-to end and end-to-side at intrafascicular fibre terminations (IFTs)<sup>18,19</sup> or as blocks of non-overlapping fibres separated by fibrous sheets called tendinous intersections (TIs)<sup>20</sup>. IFTs are known to contain dystrophin<sup>18</sup>, while TIs are of unknown composition but bear a striking structural resemblance to the dystrophin-dependent attachments we describe here, raising the possibility of molecular similarities in formation and function. In the light of our data, the presence of dystrophin at fibre end attachments in larger mammalian muscles raises the possibility that their failure contributes to the pathology of DMD. A potential mechanism for this is that the detachment of end-to-side junctions could result in the characteristic membrane tearing found along the length of fibres in DMD and subsequent degeneration. If failure at such sites were a primary pathological mechanism in dystrophinopathies, their differential deployment and failure would account for both the apparent correlation between the size of a mammal and the severity of its phenotype, and the variation in pathology between muscle groups within either DMD patients or *mdx* mice.

We demonstrate here for the first time that dystrophin is required for the stability of vertebrate muscle attachments and that muscle detachment is the primary cause of degeneration in a model of a muscular dystrophy. It is therefore possible that *sap* mutants provide a model for the novel pathological mechanism of junctional failure that could have been hitherto overlooked in DMD and other muscular dystrophies. These results suggest that the zebrafish *sap* mutant is an ideal model system for understanding the role of the dystrophin complex at muscle attachments and their failure

in muscular dystrophies, and for beginning to approach the question of relevant therapies.

#### COMMENTS

5        The externally-developing, transparent zebrafish embryo allows inspection of living muscle and the isolation of mutations affecting its formation and maintenance. A class of mutations has been identified in which normal differentiation of skeletal muscle is followed by degeneration reminiscent of human muscular dystrophies<sup>1</sup>. Here we show that one of these, *sapje* (*sap*), disrupts the zebrafish orthologue<sup>2</sup> of the human 10 *dystrophin* gene, mutations of which result in Duchenne and Becker muscular dystrophies (DMD, BMD). In mammals, dystrophin is required to link the actin cytoskeleton with the extracellular matrix between muscle fibres<sup>3</sup>. It is thought that its loss from the dystrophin glycoprotein complex (DGC) in skeletal muscle of DMD patients weakens lateral inter-fibre linkages allowing tearing of the sarcolemma, or cell 15 membrane, along the length of fibres. Surprisingly, we find that within the zebrafish embryo, dystrophin localises exclusively to the ends of muscle fibres at a site that we have defined as the embryonic myomuscular junction (MMJ). Furthermore, we show that the dystrophic phenotype of *sap* mutants is characterised by the detachment of fibre ends from this site and loss of fibre membrane integrity. Although a functional role for 20 dystrophin in maintaining junctional integrity of muscle fibres has long been postulated, direct evidence for such a role has been lacking. This mutation may therefore provide a model for a novel pathological mechanism in DMD and other dystrophies.

It will be appreciated by persons skilled in the art that numerous variations and/or modifications may be made to the invention as shown in the specific embodiments without departing from the spirit or scope of the invention as broadly described. The present embodiments are, therefore, to be considered in all respects as illustrative and 5 not restrictive.

Dated this 19th day of March 2003

Victor Chang Cardiac Research Institute Limited  
Patent Attorneys for the Applicant:  
ALLENS ARTHUR ROBINSON  
PATENT & TRADE MARKS ATTORNEYS

## REFERENCES

1. Granato, M. et al. Genes controlling and mediating locomotion behavior of the zebrafish embryo and larva. *Development* 123, 399-413 (1996).
2. Bolanos-Jimenez, F. et al. Molecular cloning and characterization of dystrophin and Dp71, two products of the Duchenne Muscular Dystrophy gene, in zebrafish. *Gene* 274, 217-226 (2001).
3. Spence, H. J., Chen, Y. J. & Winder, S. J. Muscular dystrophies, the cytoskeleton and cell adhesion. *BioEssays* 24, 542-552 (2002).
4. Higashijima, S., Okamoto, H., Ueno, N., Hotta, Y. & Eguchi, G. High-frequency generation of transgenic zebrafish which reliably express GFP in whole muscles or the whole body by using promoters of zebrafish origin. *Dev Biol* 192, 289-299 (1997).
5. Roy, M. N., Prince, V. E. & Ho, R. K. Heat shock produces periodic somitic disturbances in the zebrafish embryo. *Mech Dev* 85, 27-34 (1999).
6. Chambers, S. P. et al. Dystrophin in adult zebrafish muscle. *Biochem. Biophys. Res. Commun.* 286, 478-483 (2001).
7. Waterman, R. E. Development of the lateral musculature in the teleost, *Brachydanio rerio*: a fine structural study. *Am. J Anat.* 125, 457-493 (1969).
8. Henry, M. D. & Campbell, K. P. Dystroglycan inside and out. *Curr. Opin. Cell Biol.* 11, 602-607 (1999).
9. Parsons, M. J., Campos, I., Hirst, E. M. & Stemple, D. L. Removal of dystroglycan causes severe muscular dystrophy in zebrafish embryos. *Development* 129, 3505-3512 (2002).
10. Hamer, P. W., McGeachie, J. M., Davies, M. J. & Grounds, M. D. Evans Blue Dye as an in vivo marker of myofibre damage: optimising parameters for detecting initial myofibre membrane permeability. *J. Anat.* 200, 69-79 (2002).
11. Altschul, S. F. et al. Gapped BLAST and PSI-BLAST: a new generation of protein database search programs. *Nucleic Acids Res.* 25, 3389-3402 (1997).
12. Sitnik, R. et al. Novel point mutations in the dystrophin gene. *Hum. Mutat.* 10, 217-222 (1997).
13. Xu, X. et al. Cardiomyopathy in zebrafish due to mutation in an alternatively spliced exon of titin. *Nat. Genet.* 30, 205-209 (2002).

14. Cullen, M. J. & Jaros, E. Ultrastructure of the skeletal muscle in the X chromosome-linked dystrophic (mdx) mouse. Comparison with Duchenne muscular dystrophy. *Acta Neuropathol. (Berl)* 77, 69-81 (1988).

15. Sicinski, P. et al. The molecular basis of muscular dystrophy in the mdx mouse: a point mutation. *Science* 244, 1578-1580 (1989).

16. Deconinck, A. E. et al. Utrophin-dystrophin-deficient mice as a model for Duchenne muscular dystrophy. *Cell* 90, 717-727 (1997).

17. Grady, R. M. et al. Skeletal and cardiac myopathies in mice lacking utrophin and dystrophin: a model for Duchenne muscular dystrophy. *Cell* 90, 729-738 (1997).

18. Paul, A. C., Sheard, P. W., Kaufman, S. J. and Duxson, M. J. Localization of alpha7 integrins and dystrophin suggests potential for both lateral and longitudinal transmission of tension in large mammalian muscles. *Cell Tissue Res.* 308, 255-265 (2002).

19. Snobl, D., Binaghi, L. E. & Zenker, W. Microarchitecture and innervation of the human latissimus dorsi muscle. *J. Reconstr. Microsurg.* 14, 171-177 (1998).

20. Hijikata, T. & Ishikawa, H. Functional morphology of serially linked skeletal muscle fibers. *Acta Anat. (Basel)* 159, 99-107 (1997).

21. Macdonald, R. et al. The Pax protein Noi is required for commissural axon pathway formation in the rostral forebrain. *Development* 124, 2397-2408 (1997).

22. Higgins, D. G., Thompson, J. D. & Gibson, T. J. Using CLUSTALW for multiple sequence alignments. *Methods in Enzymology* 266, 383-402 (1996).

23. Saitou, N. & Nei, M. The neighbor-joining method: a new method for reconstructing phylogenetic trees. *Molecular Biology of Evolution* 4, 406-425 (1987).

24. Dopazo, J. Estimating errors and confidence intervals for branch lengths in phylogenetic trees by a bootstrap approach. *Journal of Molecular Evolution* 38, 300-304 (1994).

25. Kumar, S., Tamura, K., Kakobsen, I. B. and Nei, M. MEGA2: molecular evolutionary genetics analysis software. *Bioinformatics* 17, 1244-1245 (2001).

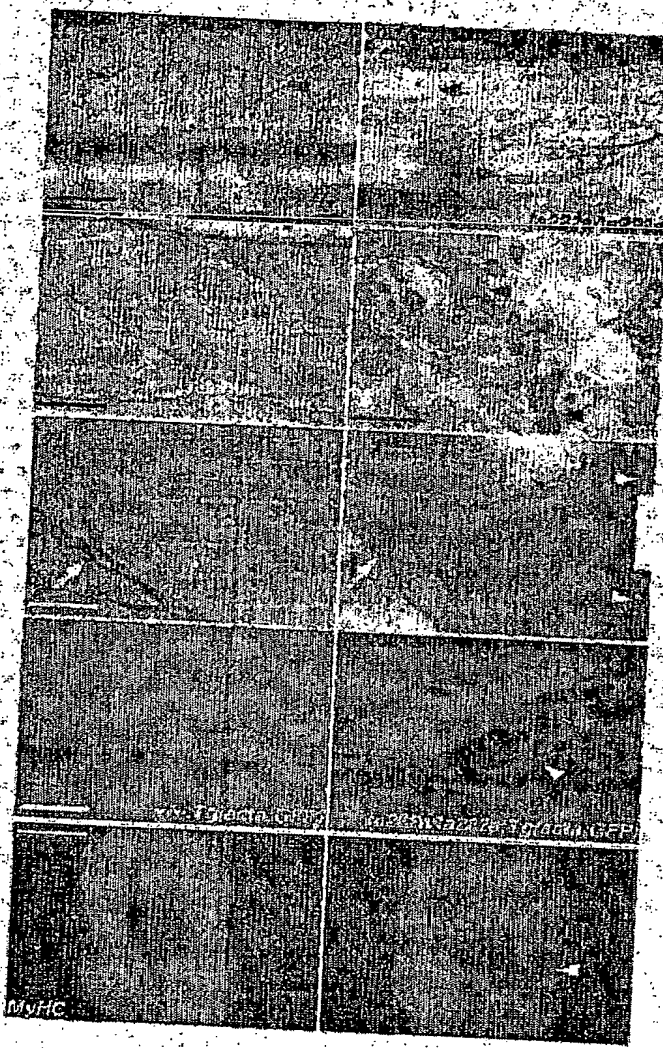


Figure 1

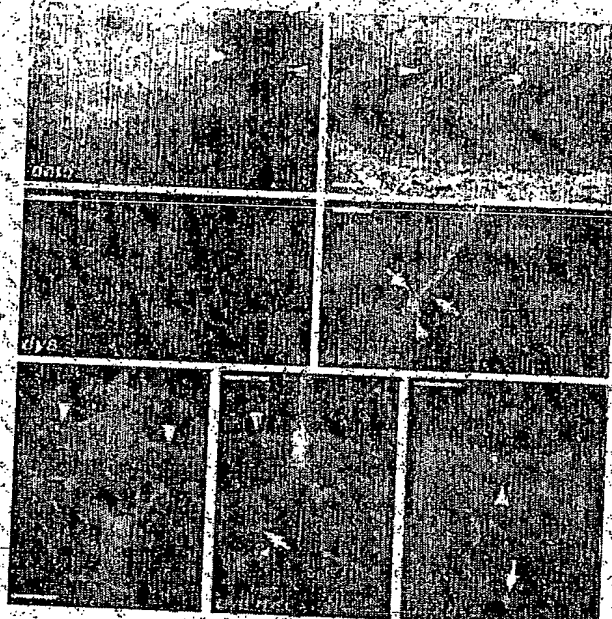


Figure 2

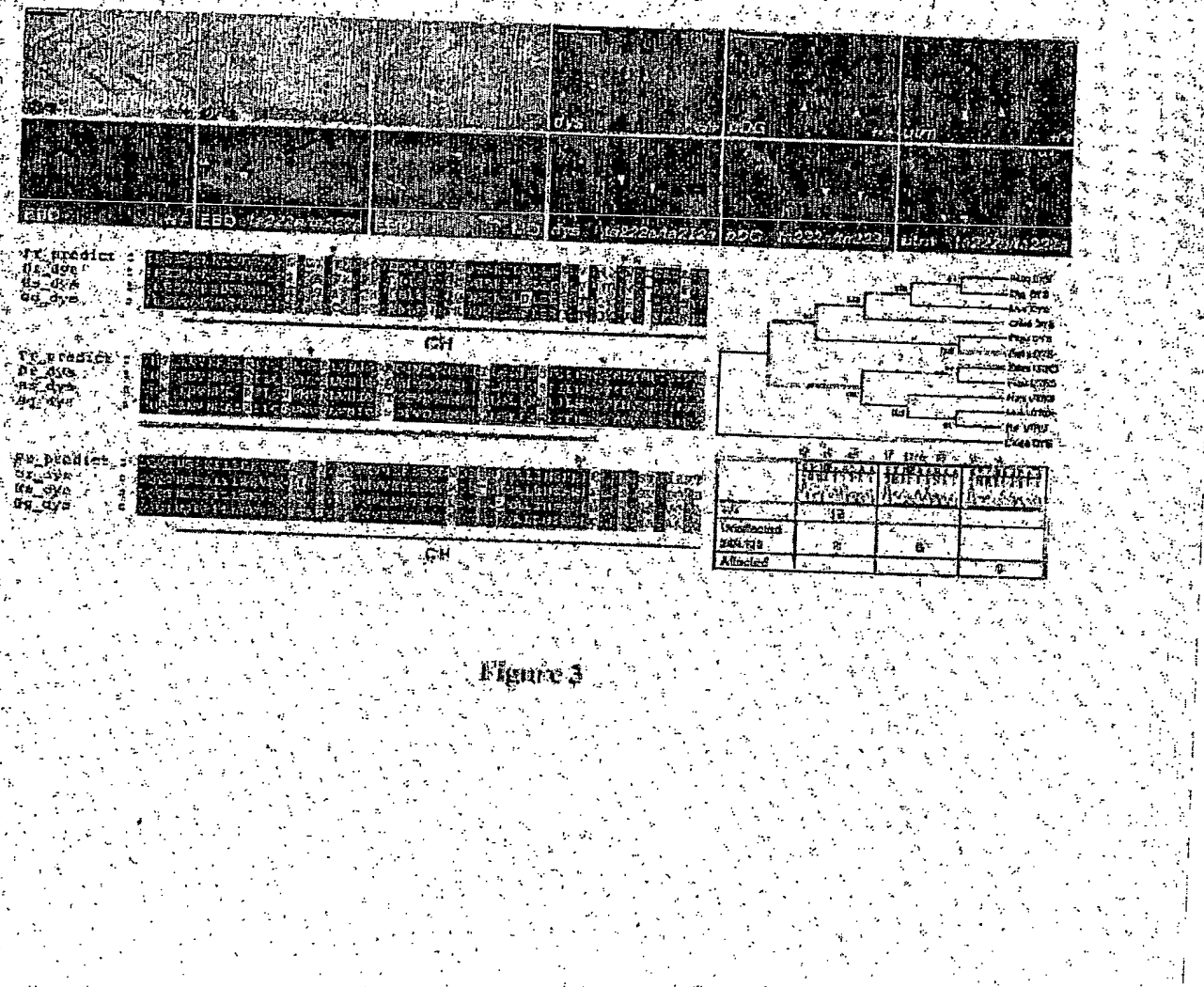


Figure 3

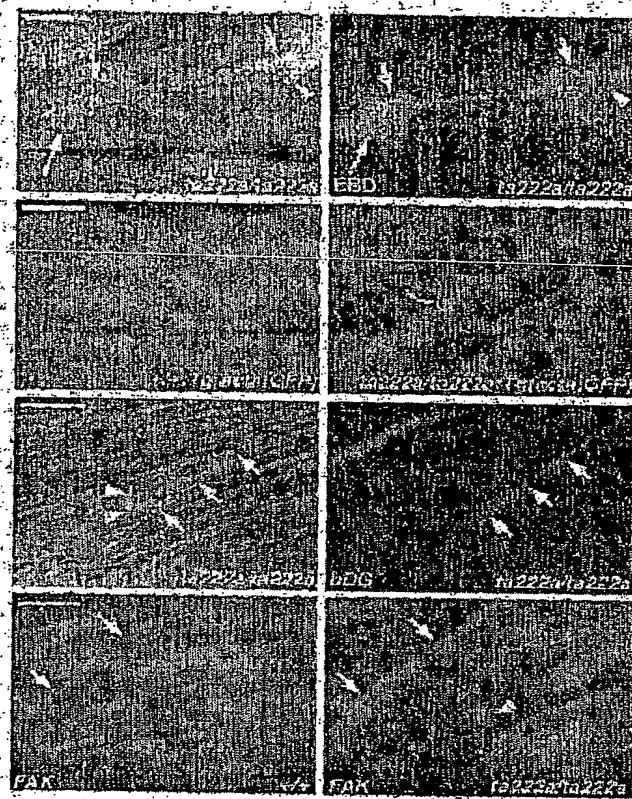


Figure 4

This Page is inserted by IFW Indexing and Scanning  
Operations and is not part of the Official Record

## **BEST AVAILABLE IMAGES**

Defective images within this document are accurate representations of the original documents submitted by the applicant.

Defects in the images include but are not limited to the items checked:

- BLACK BORDERS
- IMAGE CUT OFF AT TOP, BOTTOM OR SIDES
- FADED TEXT OR DRAWING
- BLURED OR ILLEGIBLE TEXT OR DRAWING
- SKEWED/SLANTED IMAGES
- COLORED OR BLACK AND WHITE PHOTOGRAPHS
- GRAY SCALE DOCUMENTS
- LINES OR MARKS ON ORIGINAL DOCUMENT
- REPERENCE(S) OR EXHIBIT(S) SUBMITTED ARE POOR QUALITY
- OTHER: \_\_\_\_\_

**IMAGES ARE BEST AVAILABLE COPY.**  
**As rescanning documents *will not* correct images**  
**problems checked, please do not report the**  
**problems to the IFW Image Problem Mailbox**